

1 *Manuscript for: **Electrochimica Acta***

2

3

4

5 **Kinetics of electrochemical Eu^{3+} to Eu^{2+} reduction in aqueous media**

6

7 Meryem Ozge Arman^{a,b}, Bart Geboes^{a,*}, Karen Van Hecke^a, Koen Binnemans^b, Thomas
8 Cardinaels^{a,b}

9

10 ^a Belgian Nuclear Research Centre (SCK CEN), Institute for Nuclear Materials Science,
11 Boeretang 200, B-2400 Mol, Belgium

12 ^b KU Leuven, Department of Chemistry, Celestijnenlaan 200F, P.O. 2404, B-3001 Leuven,
13 Belgium

14 *Corresponding author

15

16 Meryem Ozge Arman: meryem.arman@sckcen.be

17 ORCID ID: 0000-0002-2669-5133

18 *Bart Geboes: bart.geboes@sckcen.be

19 ORCID ID: 0000-0003-3523-5064

20 Karen Van Hecke: karen.van.hecke@sckcen.be

21 ORCID ID: 0000-0002-7100-192X

22 Koen Binnemans: koen.binnemans@kuleuven.be

23 ORCID ID: 0000-0003-4768-3606

24 Thomas Cardinaels: thomas.cardinaels@sckcen.be

25 ORCID ID: 0000-0002-2695-1002

26

27

28

29 **Abstract**

30

31 All lanthanides have a stable trivalent oxidation state, but some of them can also occur in the
32 divalent or tetravalent state. Europium is well-known for its divalent oxidation state, which
33 has been investigated in aqueous, organic, and molten salt media. In contrast to other
34 lanthanides, Eu^{3+} can be easily reduced ($E^{\circ}=-0.34$ V vs. SHE) via chemical, electrochemical or
35 photochemical routes, and Eu^{2+} is quite stable in a variety of electrolytes, including nitrate
36 salts. To date, the kinetics of the $\text{Eu}^{3+}/\text{Eu}^{2+}$ reduction reaction has been investigated only by
37 polarography and chronopotentiometry, most often in perchlorate medium. In this study, the
38 kinetics of the $\text{Eu}^{3+}/\text{Eu}^{2+}$ couple were analysed in nitrate, chloride and perchlorate media by
39 cyclic voltammetry and linear sweep voltammetry with a rotating disk electrode (RDE). The
40 diffusion coefficient, charge transfer coefficient and rate constants were calculated based on
41 the Levich and Koutecký-Levich analysis and Tafel plot to gain insight in the electrochemical
42 process and the influence of the electrolyte type on it. Given the pre-existing characterization
43 of this redox couple in perchlorate medium, it is selected as a reference system to both
44 compare the kinetic parameters and to validate whether the methodology can be applied to
45 other electrolytes. The Eu^{3+} reduction reaction was found to be quasi-reversible in these
46 electrolytes and the calculated kinetic parameters are in line with the previously reported
47 values.

48

49

50

51 **Keywords:** aqueous electrolytes; divalent europium; lanthanides; rare earths; rotating disk
52 electrode

53 1. Introduction

54

55 Lanthanide chemistry is dominated by the trivalent oxidation state and by the gradual filling
56 of the 4f shell across the lanthanide series. However, some lanthanides display unusual
57 oxidation states in the series such as cerium(IV), praseodymium(IV), terbium(IV), samarium(II),
58 europium(II) and ytterbium(II). The divalent europium ion is well characterized, thanks to the
59 facts that the reduction potential of the $\text{Eu}^{3+}/\text{Eu}^{2+}$ couple is readily accessible ($E^\circ(\text{Eu}^{3+}/\text{Eu}^{2+}) =$
60 -0.34 V), and that the divalent oxidation state is relatively stable due to a half-filled 4f subshell.
61 The electrochemical behavior of lanthanide elements has been extensively studied as model
62 systems in various electrolyte conditions, such as molten salts, ionic liquids, and aqueous/non-
63 aqueous solutions [1–14].

64 The reduction of Eu^{3+} has been investigated using chemical, photochemical and
65 electrochemical approaches [11,14–21]. The kinetics of the electrochemical reduction
66 reaction have also been investigated using several methods such as polarography,
67 chronoamperometry or voltammetry [22–31]. In earlier works, the kinetics of Eu^{3+} reduction
68 were investigated in aqueous formamide and perchlorate media using a dropping mercury
69 electrode to understand the electrochemical behavior of the system and the influence of
70 viscosity and temperature [29–33]. In these media, the kinetic parameters transfer coefficient
71 (α) and rate constant (k) of the reaction as well as the diffusion coefficient (D) have been
72 calculated. The influence of the formamide concentration on the reversibility was discussed
73 as well as that of the viscosity and pH. In these media, inner-sphere complexation is not very
74 pronounced and Eu^{3+} ions are present mainly in hydrated form. However, with increasing
75 concentration of the electrolyte, a negative shift of the peak potential occurs, which can be
76 explained by the decrease of the solvent activity and lowering the hydration of the europium
77 ions in solution, increasing the entropy. This results in a higher stability of Eu^{2+} complexes

78 [21,31]. Furthermore, the reduction of Eu^{3+} has also been investigated in chloride and nitrate
79 media, with the aim to develop efficient separation processes by change of oxidation state of
80 europium [16,18–20,34–37]. Van de Voorde *et al.* reported that at high aqueous nitrate
81 concentrations, Eu^{3+} can efficiently be electrochemically reduced to Eu^{2+} and that the Eu^{2+} ion
82 is very stable in this system [21]. The Eu^{3+} reduction kinetics and mechanism were also
83 investigated in hydrochloric acid solutions by Atanasyants *et al.* and these authors concluded
84 that the process occurs in the mixed kinetics region [28]. In both studies of Van de Voorde *et*
85 *al.* and Atanasyants *et al.*, a graphite electrode was used instead of a mercury one, and the
86 reactions were found to be quasi-reversible to irreversible based on the electrolyte and the
87 concentrations [21,28]. The effect of non-aqueous solvents such as propylene carbonate and
88 ethylene glycol on the reduction kinetics of Eu^{3+} were also investigated. The kinetic
89 parameters were obtained via chronopotentiometry using a mercury electrode. The Eu^{2+}
90 complexes were found to be stable, but water impurities decreased the stability [10,38]. The
91 aim to gain further insight in the electron transfer reaction of Eu^{3+} reduction led to the use of
92 room-temperature ionic liquids [39] and mixed solvents [40]. Based on this knowledge new
93 electrode materials such as bismuth single-crystal or boron-doped-diamond thin film
94 electrode were tested for the $\text{Eu}^{3+}/\text{Eu}^{2+}$ redox couple to gain fundamental insight in the
95 electron-transfer kinetics on solid-state electrodes [22,24].

96 Present work is a fundamental study on the reduction kinetics of europium(III) with a
97 conventional solid-state electrode, by cyclic voltammetry and linear sweep voltammetry with
98 a rotating disk electrode (RDE). This work is the first study using a controlled convection
99 method for europium reduction kinetics. Multiple electrolytes such as perchlorate, chloride
100 and nitrate were tested and the results were compared with the existing literature data for
101 perchlorate media. Given the extensive use of these media in literature, which were

102 investigated by various techniques, nitrate, chloride and perchlorate media were chosen for
103 this fundamental study to validate the applicability of the technique used in the present work.
104 As discussed earlier, the $\text{Eu}^{3+}/\text{Eu}^{2+}$ redox couple has been studied extensively in various
105 electrolytes and has been used to explore new electrode materials. However the kinetic study
106 has not been explored for nitrate media yet, and most often a mercury electrode was applied.
107 To gain a better insight in the system, the electrochemical reduction of Eu^{3+} is investigated in
108 three different media: perchlorate, chloride, and nitrate. Cyclic voltammetry and linear sweep
109 voltammetry are performed using a glassy carbon rotating disk electrode under stationary or
110 rotating conditions.

111 **2. Experimental**

112 **2.1. Materials** 113

114 $\text{Eu}(\text{NO}_3)_3 \cdot 6\text{H}_2\text{O}$ (99.9%), $\text{EuCl}_3 \cdot 6\text{H}_2\text{O}$ (99.9%) and $\text{Eu}(\text{ClO}_4)_3$ in aqueous solution (50%) were
115 purchased from Strem Chemicals, Inc. (Newburyport, USA). $\text{Ca}(\text{NO}_3)_2 \cdot 4\text{H}_2\text{O}$ ($\geq 99\%$), $\text{CaCl}_2 \cdot 6\text{H}_2\text{O}$
116 (98%) and NaClO_4 ($\geq 98\%$) are purchased from Sigma-Aldrich (Overijse, Belgium). All products
117 were used as received, without any further purification. Aqueous samples are prepared with
118 Milli Q water ($18.2 \text{ M}\Omega \cdot \text{cm}$ at $25 \text{ }^\circ\text{C}$).

119 **2.2. Instruments and electrodes** 120

121 A three-electrode electrochemical cell was used for the electrochemical reduction of
122 europium. The potential was controlled using a Metrohm Autolab PGSTAT302N potentiostat
123 in potentiostatic mode, controlled by Nova 2.1.5 software. The rotating disk electrode (RDE)
124 experiments were conducted with an AUTOLAB RDE2 rotator with the rotation speed (100 to
125 10000 rpm), remotely controlled by the Nova software. A custom-made glass electrochemical
126 cell with 100 mL inner capacity was used for the voltammetry tests. Prior to the

127 measurements, the solution was purged with argon gas. Experiments were conducted while
128 an inert gas blanket was created by maintaining a continuous argon flow over the solution.
129 The working electrode was a glassy carbon disk ($\varnothing = 3$ mm), the counter electrode was a coiled
130 platinum wire ($\varnothing = 1$ mm) and the reference electrode was Ag/AgCl in 3 mol.L⁻¹ KCl. Prior to
131 the measurements, the electrodes were cleaned first with 3 mol.L⁻¹ HNO₃, and then methanol.
132 Solutions containing 10 mmol.L⁻¹ Eu³⁺ in 0.1 mol.L⁻¹ nitrate, perchlorate or chloride media were
133 used as electrolytes. Higher concentrations of the electrolytes were avoided due to inhibition
134 occurring on the working electrode.

135 **3. Results and discussion**

136 **3.1. Cyclic voltammetry**

137

138 Cyclic voltammetry (CV) was used to investigate the redox behavior of Eu³⁺ / Eu²⁺ in aqueous
139 nitrate, chloride and perchlorate solutions, as well as to determine the reduction potentials
140 as a function of the electrolyte composition. These experiments were performed using 10
141 mmol.L⁻¹ of Eu³⁺ salt containing the same anion as the electrolytes. The electrolyte
142 concentrations were 0.1 mol.L⁻¹ for nitrate and chloride, and 1 mol.L⁻¹ for perchlorate media.
143 The voltammograms were recorded in various scan rates in range 10 – 1000 mV.s⁻¹. The blank
144 electrolytes were measured as well to validate that the electrochemical activity was
145 originating uniquely from Eu³⁺ complexes (ESI Fig 1, Fig 2 and Fig 3).

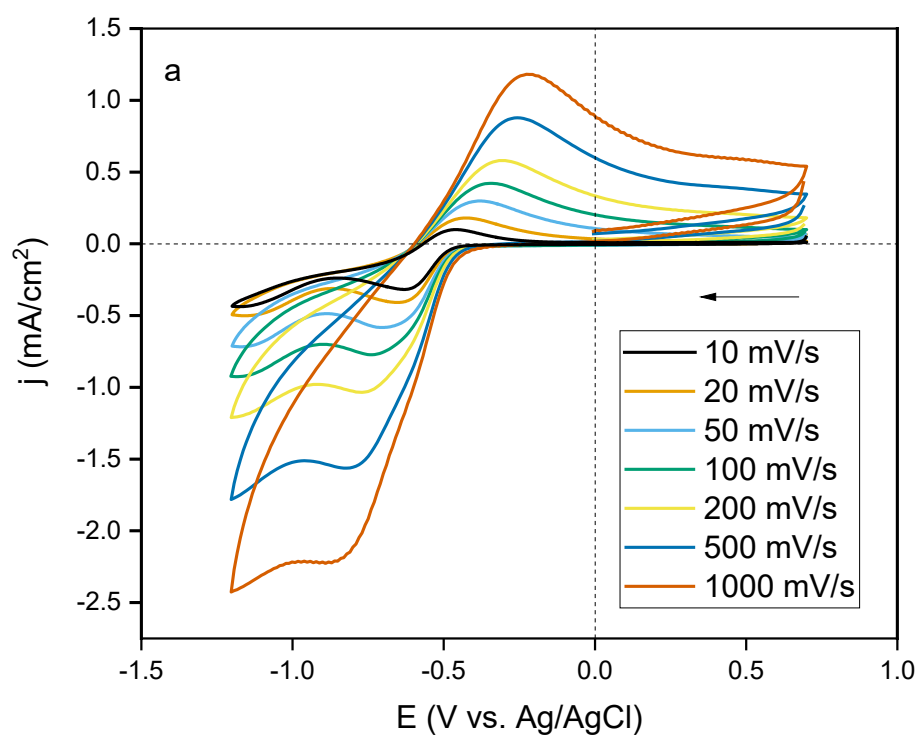
146 The influence of complexation in these electrolytes can be mainly explained by the change in
147 hydration number and the inner/outer sphere coordination environment resulting in different
148 reduction potentials. The formal reduction potential of a redox compound is affected by the
149 interaction with ligands, i.e. the coordination of Eu³⁺ and Eu²⁺ and is a function of the ligand
150 dissociation constants [41]. In addition, changing the electrolyte concentration leads to a

151 considerable difference in activity, ionic strength and hydration of the ions in solution, thus
152 changing their inner coordination sphere. Europium ions are strongly hydrated in aqueous
153 media because of their high charge densities, with the highest charge density for trivalent
154 europium, which is known to be coordinated by 8 to 9 water molecules, whereas divalent
155 europium is coordinated by 7 to 8 water molecules. Chloride and nitrate show only modest
156 levels of association with lanthanide ions in aqueous solutions, mostly in the form of double-
157 solvent-separated ion pairs. Therefore, they are found to predominantly form outer-sphere
158 complexes, even at high salt concentrations. Thus, Eu^{3+} and Eu^{2+} ions in aqueous media can
159 be considered fully hydrated ions.

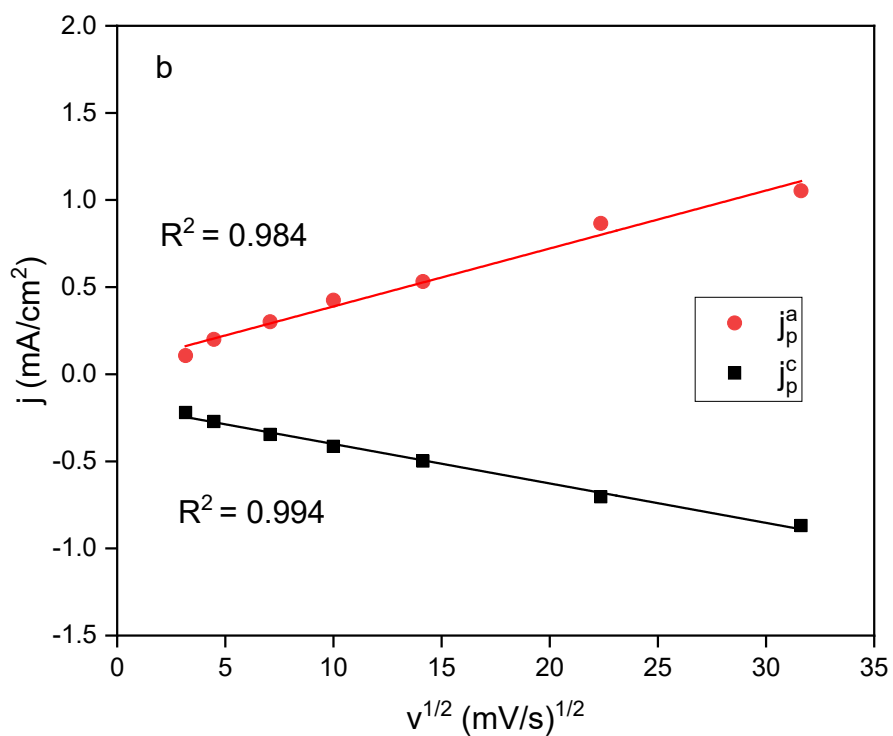
160 The reduction of Eu^{3+} to Eu^{2+} was achieved in the electrolytes consisting of nitrate, chloride
161 and perchlorate ions in quasi-neutral pH [21,31]. In the work of Van de Voorde *et al.* [21], both
162 chemical and electrochemical reduction of Eu^{3+} to Eu^{2+} were performed at the pH of the
163 solutions between 4 and 6.5 to avoid re-oxidation of Eu^{2+} by H^+ as well as the pH would be
164 sufficiently low to prevent hydrolysis of Eu^{3+} . In addition, Rabockai *et al.* [29] discussed the
165 influence of pH on the reduction of europium pair in $1 \text{ mol.L}^{-1} \text{ NaClO}_4$ in the presence of
166 formamide using chronoamperometry on mercury electrode. It was reported that the pH
167 effect was absent when solutions containing more than 70% formamide at all concentrations
168 of Eu^{3+} were used, indicating that the reversibility of the reaction was independent on pH.
169 However, at low concentrations of formamide (0 – 30%), the calculated kinetic parameters
170 showed that the reaction was quasi-reversible, and mainly the anodic reaction was influenced
171 more by pH compared to the cathodic process [29]. In the current work, based on these
172 information, the pH of the solutions were kept ~ 4 and not further manipulated.

173 Fig. 1, Fig. 2, and Fig. 3 show the cyclic voltammograms of Eu^{3+} in perchlorate, nitrate and
174 chloride media as a function of the potential sweep rate at a glassy carbon disk electrode. In
175 all three media, a linear relationship between the cathodic peak currents and scan rate was
176 observed, indicating a diffusion-controlled charge transfer. When the peak separation
177 potentials are plotted as a function of potential sweep rate in logarithmic scale, as can be seen
178 in Fig. 4, a linear relationship (with $0.991 \leq R^2 \leq 0.996$) is found for all electrolytes.

179 Only minor differences in the peak potentials at different electrolyte solutions were observed,
180 as can be seen in Fig. 1, Fig. 2, and Fig. 3. At a sweep rate of $50 \text{ mV}\cdot\text{s}^{-1}$, the cathodic peak
181 potentials (E_p^c) are: -0.65, -0.68 and -0.68 V vs. Ag/AgCl, whereas the anodic peak potentials
182 (E_p^a) are -0.40, -0.44 and -0.38 V vs. Ag/AgCl for perchlorate, nitrate and chloride media,
183 respectively. The differences between the cathodic and anodic peak potentials are given in
184 Table 1. Since these differences are larger than 59 mV in all media, and the E_p values change
185 as a function of the scan rate, the reduction reaction in these electrolytes can be considered
186 as being quasi-reversible.



187

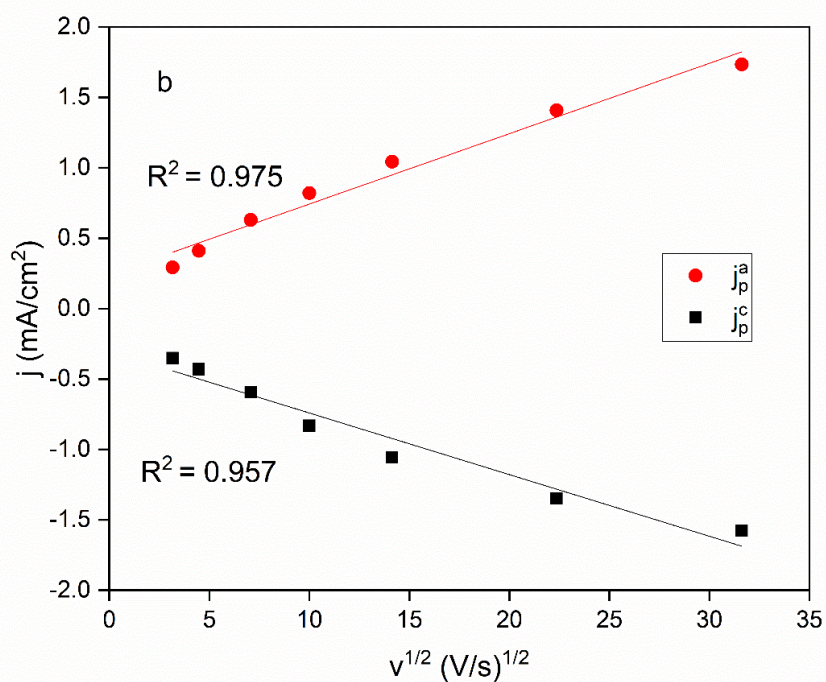
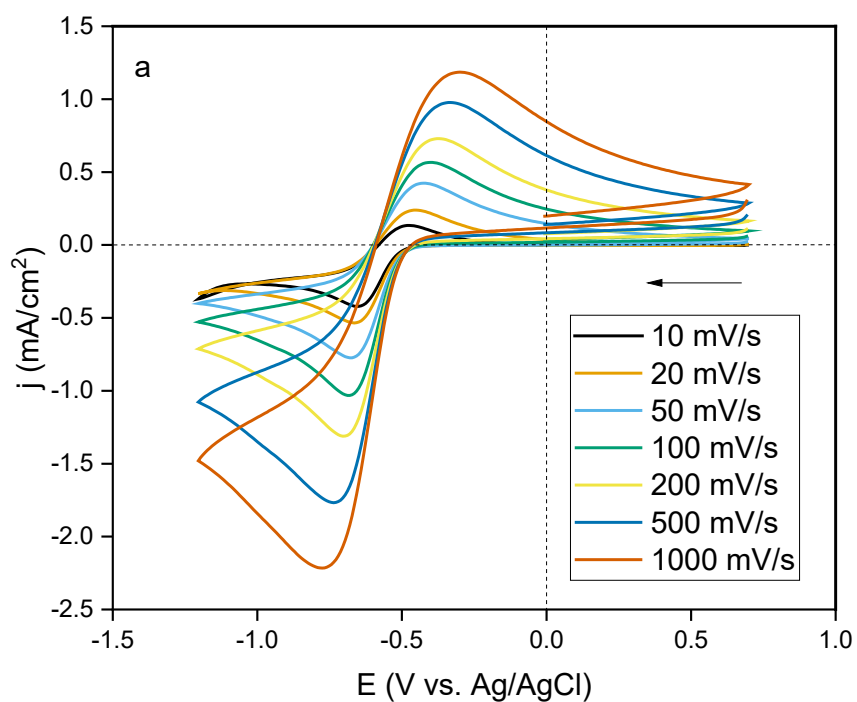


188

189 Fig. 1. a) Cyclic voltammograms (second cycles) of 10 mmol.L⁻¹ Eu³⁺ in 1 mol.L⁻¹ NaClO₄ at various scan rates

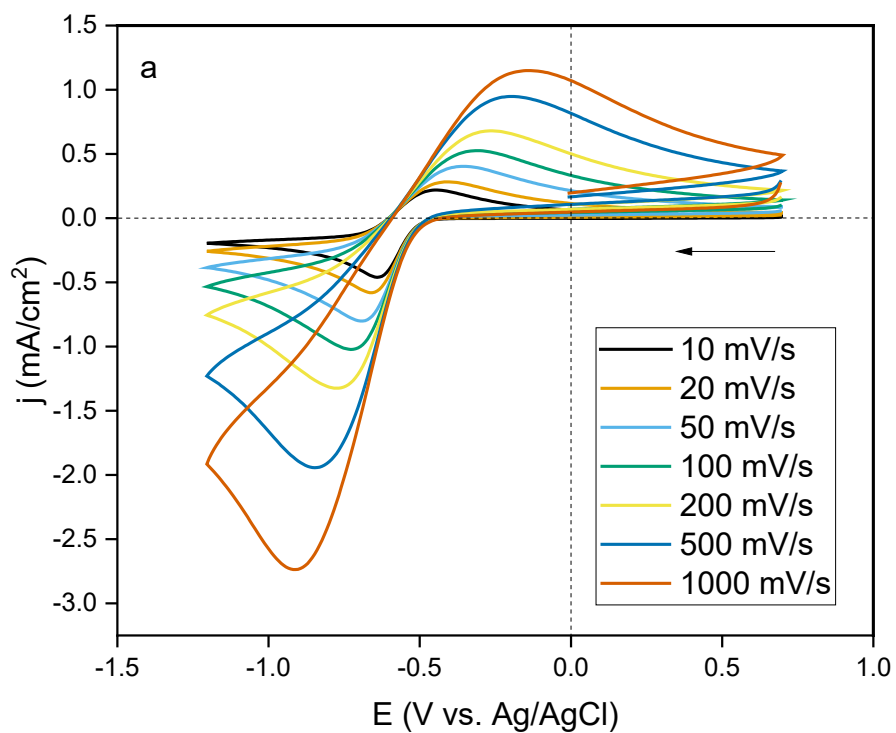
190 between 10-1000 mV/s b) Linear correlation of anodic and cathodic peak densities with respect to the square

191 root at these scan rates.

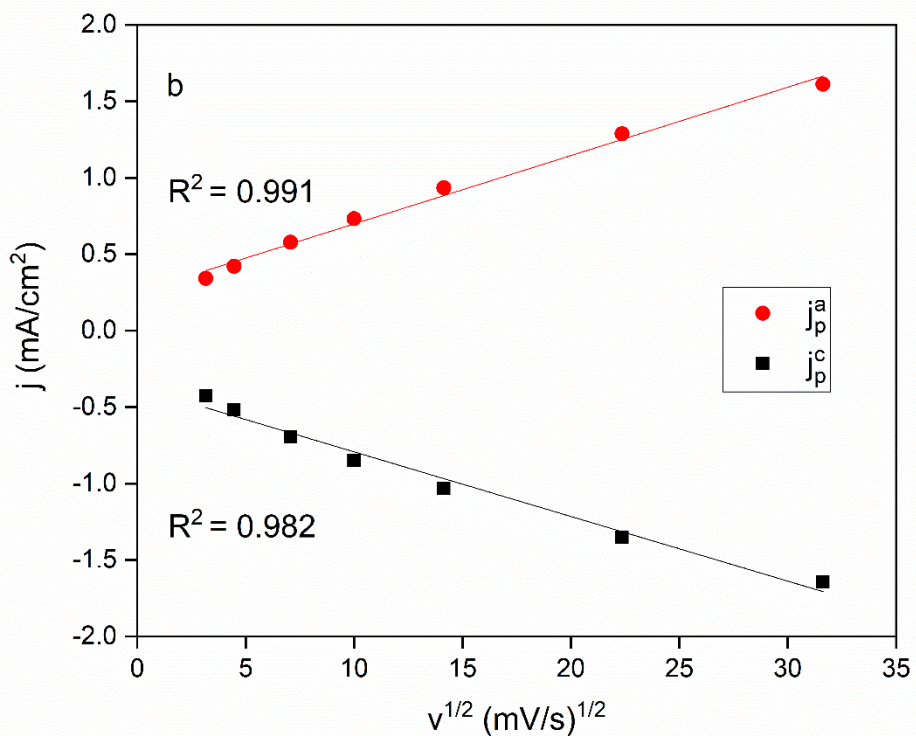


192

193 Fig. 2. a) Cyclic voltammograms (second cycles) of $10 \text{ mmol.L}^{-1} \text{ Eu}^{3+}$ in $0.1 \text{ mol.L}^{-1} \text{ Ca(NO}_3)_2$ at various scan rates
 194 between 10-1000 mV/s b) Linear correlation of anodic and cathodic peak densities with respect to the square
 195 root at these scan rates.

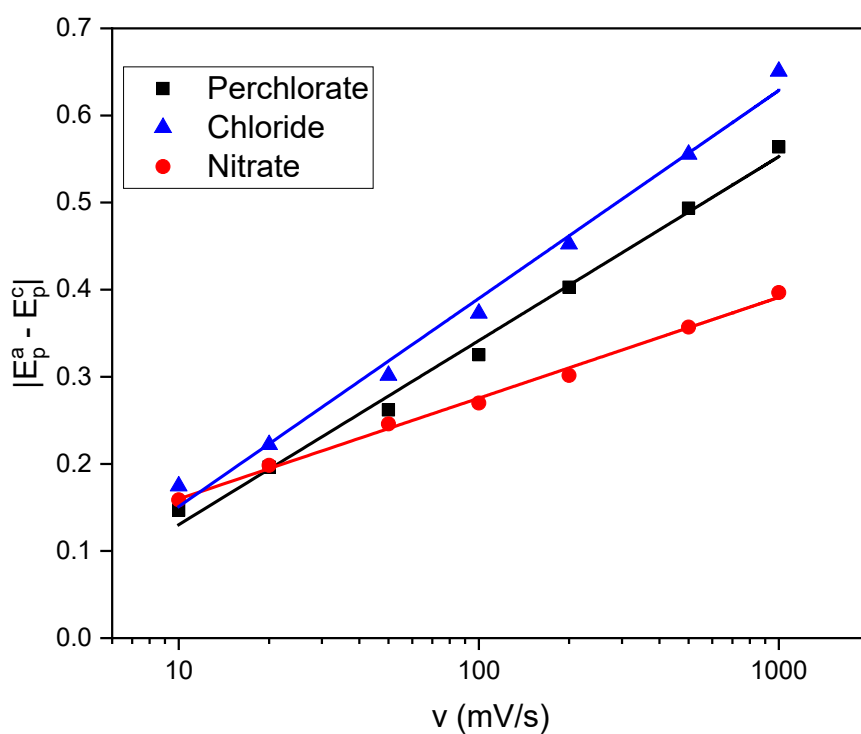


196



197

198 Fig. 3. a) Cyclic voltammograms (second cycles) of 10 mmol.L⁻¹ Eu in 0.1 mol.L⁻¹ CaCl₂ at various scan rates
 199 between 10-1000 mV/s b) Linear correlation of anodic and cathodic peak densities with respect to the square
 200 root at these scan rates.



201
 202 Fig. 4. Peak separation potentials of 10 mmol.L⁻¹ Eu³⁺ in 1 mol.L⁻¹ perchlorate, 0.1 mol.L⁻¹ chloride and 0.1
 203 mol.L⁻¹ nitrate media as a function of scan rate in logarithmic scale.

204
 205
 206 Table 1. Difference in anodic and cathodic potentials at 10 mV/s and diffusion coefficients of Eu³⁺/Eu²⁺ reaction
 207 at different electrolytes.

Medium	ΔE_p (V vs. Ag/AgCl)	$D \times 10^6$ (cm ² /s)	Reported D values $\times 10^6$ (cm ² /s)
1 mol.L ⁻¹ NaClO ₄	0.25	6.42	4.8 [42] 5.7 [30] 10 [33]
0.1 mol.L ⁻¹ Ca(NO ₃) ₂	0.25	25.3	-
0.1 mol.L ⁻¹ CaCl ₂	0.30	23.2	-

208
 209
 210

211 In aqueous chloride and nitrate media, it was observed that varying the salt concentration
 212 resulted in a shift of the reduction potential, and the reduction reaction was found to be more
 213 favorable at higher electrolyte concentrations [21]. Although the electrolyte concentration
 214 was higher in perchlorate medium, the peak potentials differed only ± 20 mV from the other
 215 electrolytes. Among these, the reduction potential was the lowest in nitrate medium, similar
 216 to the observations made by Van de Voorde *et al.*, where the oxidation and reduction of
 217 europium in nitrate aqueous media consistently have the lowest values at all concentrations
 218 [21]. Furthermore, chloride and perchlorate anions do only weakly interact with Eu^{3+} ions in
 219 aqueous media, so that only outer-sphere complexes are formed. However, Eu^{3+} nitrate
 220 solutions exhibit properties that lie between the behavior of those of weakly complexing
 221 chloride and perchlorate ions and the more strongly complexing sulfate ion [43–46].
 222 Therefore, Eu^{3+} and Eu^{2+} ions are hydrated in these electrolytes and they form dominantly
 223 outer-sphere complexes, resulting in similar reduction potentials (E_p^c of -0.65 V vs. Ag/AgCl
 224 in perchlorate, -0.68 V vs. Ag/AgCl in nitrate and -0.68 V vs. Ag/AgCl in chloride media)
 225 independently of the electrolyte.

226 The relationship between the peak current and the scan rate for reversible reactions, which is
 227 also valid for quasi-reversible reactions, is given by the Randles–Sevcik equation:

$$228 \quad i_p^c = 0.496nFCAD^{1/2} \left(\frac{(\alpha n_\alpha)Fv}{RT} \right)^{1/2} \quad (1)$$

229 where i_p^c is the cathodic peak current (in amperes), n is the number of exchanged electrons,
 230 F is the Faraday constant (96485 C. mol^{-1}), C is the europium concentration (in $\text{mol}\cdot\text{cm}^{-3}$), A
 231 is the electrode surface area (in cm^2), D is the diffusion coefficient (in cm^2s^{-1}), v is the
 232 potential sweep rate (in $\text{V}\cdot\text{s}^{-1}$), α is the charge-transfer coefficient, n_α is the number of
 233 electrons transferred in the rate-determining step, R is the universal gas constant and T is

234 the absolute temperature (in K). In all electrolytes, the linear dependence of cathodic peak
235 current to the square root of the scan rate, shows that the reduction of Eu^{3+} in these solvents
236 is diffusion-controlled (Fig. 1, Fig. 2 and Fig. 3). In order to calculate the diffusion coefficients
237 in these electrolytes, the αn_{α} value was estimated by using the half-peak potential
238 relationship equation for irreversible systems:

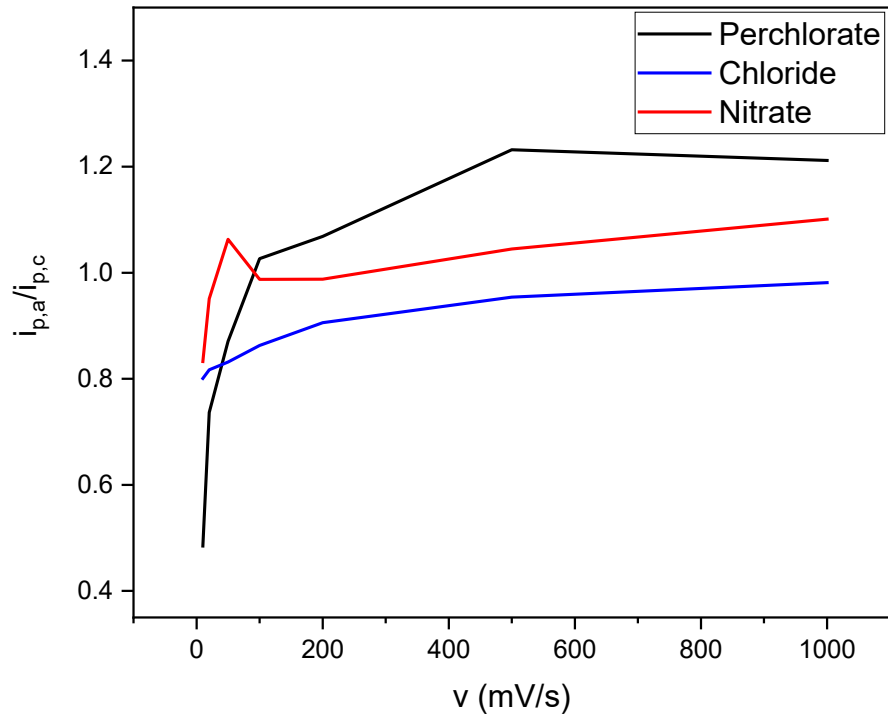
$$239 \quad \left| E_p^c - E_{\frac{p}{2}}^c \right| = \frac{1.857 RT}{\alpha n_{\alpha} F} \quad (2)$$

240 where $E_{\frac{p}{2}}^c$ is the cathodic half-peak potential. The calculated and reported D values can be
241 found in Table 1. The experimental values for the diffusion coefficient in perchlorate medium
242 are in close agreement with values reported in the literature, which were derived from
243 chronoamperometric techniques or polarography [30,38]. To the best of our knowledge, there
244 have been no studies reported in chloride or nitrate media yet, apart from the kinetic study in
245 2 mol.L^{-1} HCl by Atanasyants *et al.* who reported mixed kinetics [28]. The diffusion coefficients
246 in all media are of the same order of magnitude, slightly higher in nitrate and chloride media.
247 The difference in the concentrations would impact the viscosity of these solutions. Thus, the
248 increase in the diffusion coefficient can be attributed to the decreasing viscosity in nitrate and
249 chloride media [47].

250

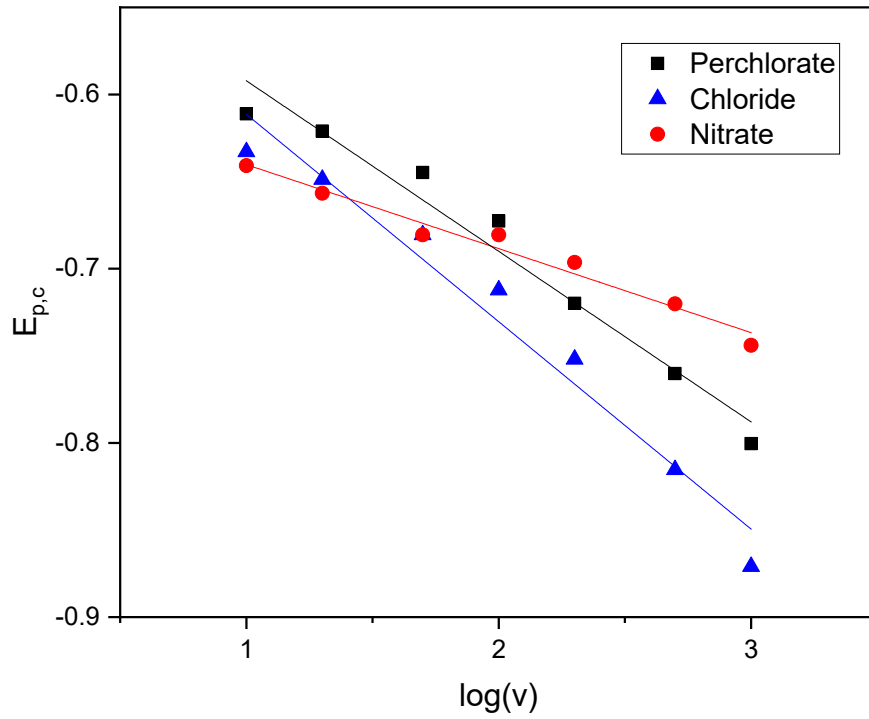
251 The reduction mechanism is further evaluated for all media by the ratio of the anodic peak
252 current to cathodic peak current with respect to scan rate (Fig. 5). In slower scan rates for the
253 perchlorate medium, the ratio is lower than 1, where with increasing scan rates the ratio
254 becomes closer to 1. This could suggest an irreversible chemical reaction paired with a
255 reversible electron transfer or an additional electrochemical redox couple overlapping the

256 potential range. In the chloride and nitrate media on the other hand, at all scan rates, the ratio
257 seems to constant and close to 1, what could indicate a single reversible electron transfer. In
258 addition, the linear correlation between $E_{p,c}$ vs. $\log(v)$ supports the EC mechanism for
259 perchlorate medium [48]. Cyclic voltammetry simulations are performed to gain further
260 insight in the possible electrochemical mechanisms of this redox couple using the CV Simulator
261 tool developed by Brown *et al.* [49] (ESI Fig 4). The kinetic parameters of the simulations are
262 presented in ESI Table 1 and show good general similarity to the experimental values obtained
263 in this study via rotating disk experiments. The fittings were performed assuming an E
264 mechanism, resulting in good agreement with the experimental voltammograms in chloride
265 and nitrate media. In perchlorate medium, no good fit could be obtained for either a single E
266 or EC mechanism. The contribution of a second electroactive species is therefore considered
267 and could correspond to the H^+ reduction reaction. Steeman *et al.* [50] observed the
268 interference of H^+ reduction at higher potentials in 1 M $NaClO_4$, overlapping with the Yb^{3+}
269 reduction region. Similar to the observations in Yb^{3+} reduction, Eu^{3+} reduction in perchlorate
270 electrolyte at moderate pH also result in the more prominent contribution of H^+ reduction at
271 lower scan rates, which could explain the lower $i_{p,a}/i_{p,c}$ values at these scan rates.



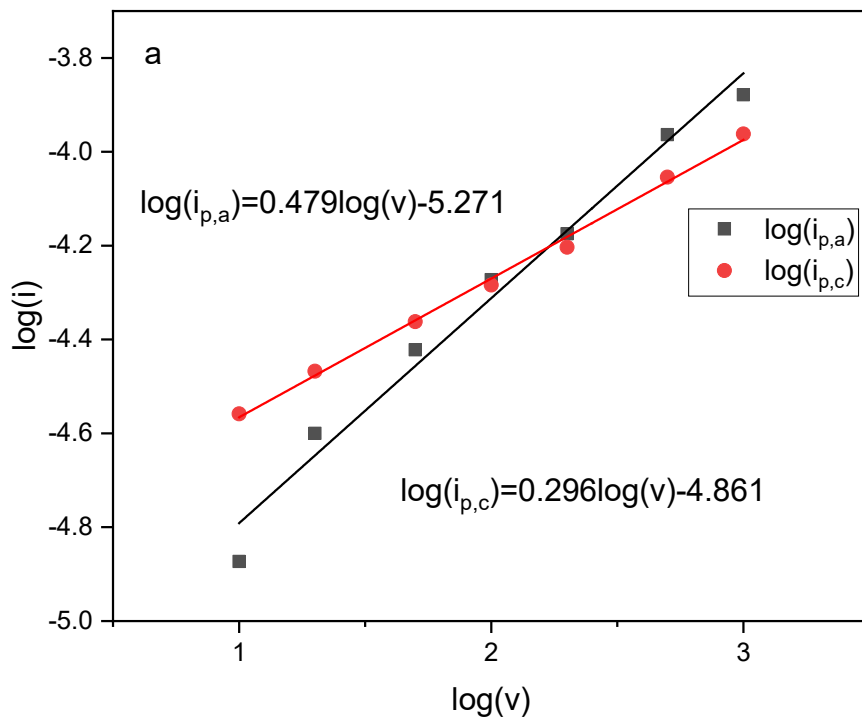
272

273 Fig. 5. Ratio of the anodic and cathodic peak currents of 10 mmol.L⁻¹ Eu³⁺ in 1 mol.L⁻¹ perchlorate, 0.1 mol.L⁻¹
274 chloride and 0.1 mol.L⁻¹ nitrate media as a function of scan rate.

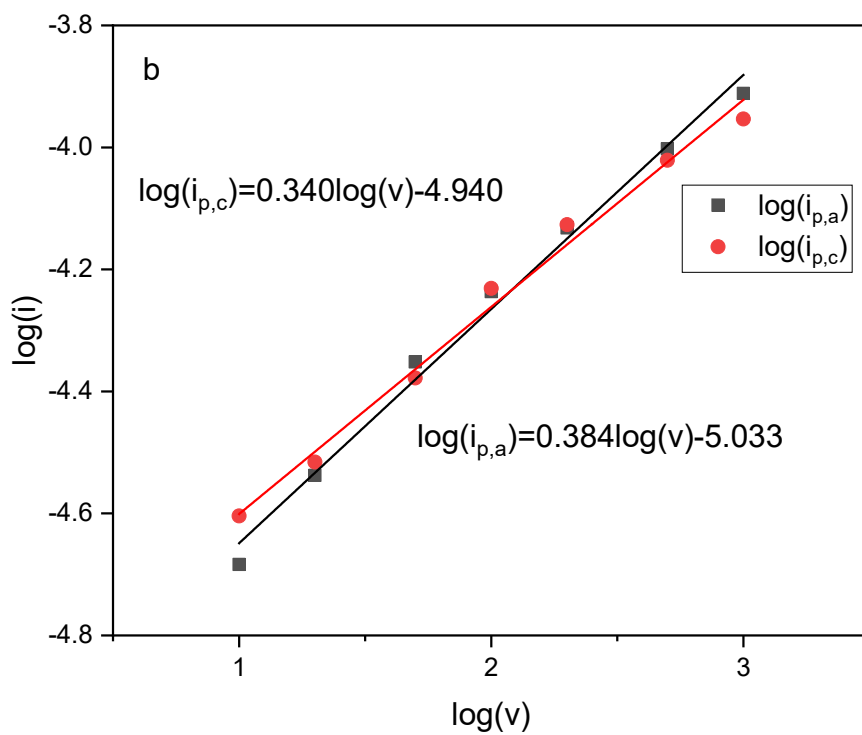


275

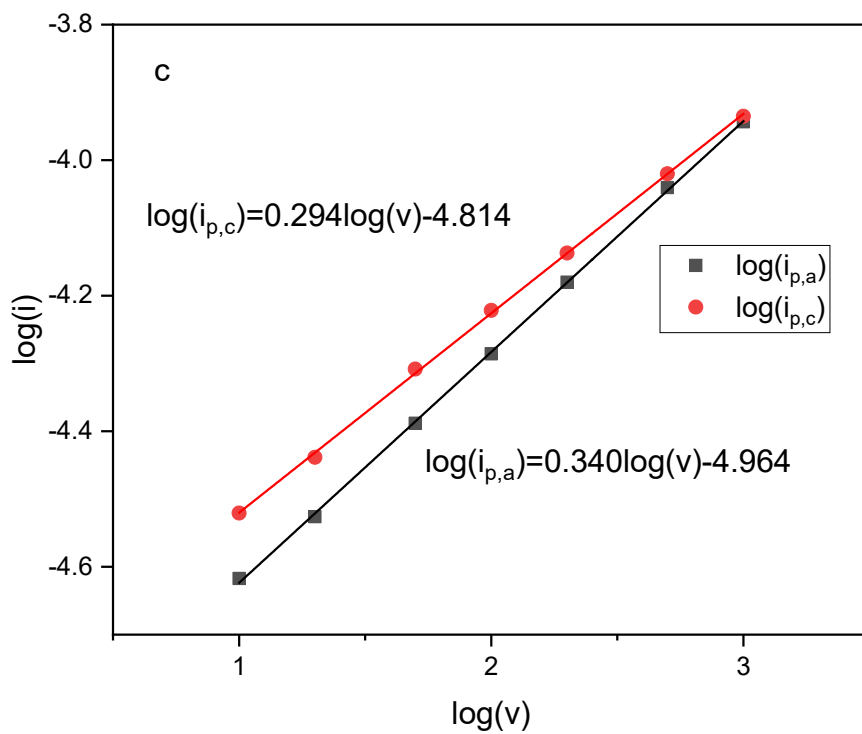
276 Fig. 6. E_p vs. log(v) graph for the voltametric peaks for perchlorate, chloride and nitrate media.



277



278



279

280 Fig. 7. Log(i) vs. log(v) graph for the voltametric peaks for a) perchlorate, b) nitrate and c) chloride media.

281

282 The linear graphs of $\log(i)$ vs. $\log(v)$ in Fig. 7 show that the process is diffusion regulated, with
283 charge transfer and mass transport both controlling the peak current [51]. The peak current
284 ratio is discovered to be significantly larger than unity, which is consistent with the results and
285 suggests that the system is quasi-reversible [47].

286

287 **3.2. Linear sweep voltammetry at rotating disk electrode**

288

289 Cyclic voltammetry is a valuable technique to qualitatively study the reactivity of compounds
290 and to learn about the potential at which redox processes occur, the oxidation states, the
291 number of electrons involved in the process, any possible chemical processes involved with
292 the electron transfer etc. However, due to its non-stationary behavior and capacitive
293 contributions involved, quantitative determination of kinetic parameters cannot be
294 determined. Therefore, to further evaluate the kinetic parameters of the Eu^{3+} reduction
295 reaction in perchlorate, nitrate and chloride media, linear sweep voltammetry at a rotating
296 disk electrode (RDE) was used. Compared to polarography or chronoamperometry, rotating
297 disk electrode experiments have advantages such as supplying more reliable mass transport
298 conditions, quickly achieving steady-state electrode currents, a well-defined electrode surface
299 for quantitative analysis and, as a result, higher sensitivity [52,53]. For these experiments, an
300 in-house made water-jacketed three electrode glass cell with 100 mL inner volume was used.
301 The solutions were purged with argon gas, at least for 30 minutes, before the experiment, and
302 during the experiment an argon blanket was supplied to avoid oxidation of Eu^{2+} by air. In order
303 to check the electrochemical activity of $\text{Eu}^{3+}/\text{Eu}^{2+}$, voltammograms were recorded at different
304 rotation speeds.

305 In previous work of Van de Voorde *et al.*, a detailed parameter study was performed on the
306 stability of Eu^{2+} as a function of the electrolyte composition, and it was found that the stability
307 of Eu^{2+} increased at higher nitrate and chloride concentrations [21]. Based on these results,
308 the initial experiments were conducted at 3 mol.L^{-1} electrolyte solutions (ESI Fig 5 and Fig 6).
309 However, at these high electrolyte concentrations, the voltammograms were not
310 reproducible, and inhibition of the glassy carbon electrode was observed at higher rotation
311 speeds. There are issues related with the use of nitrate salts as supporting electrolyte, due to
312 the possible interactions with the electrode surface, anodic reactions of nitrate ions and
313 complex formation with the ion of interest [54–56]. The inhibition of the electrode could also
314 be explained by the selective adsorption of nitrate ions on the electrode which prevents the
315 charge transfer reaction of europium. Therefore, the electrolyte concentrations was kept at
316 0.1 mol.L^{-1} or 1 mol.L^{-1} to obtain reliable results and to enable comparison of calculated kinetic
317 parameters with literature data.

318 The dependence of current density on the electrode potential is presented in the linear sweep
319 voltammograms in Fig. 5.a., Fig. 6.a. and Fig. 7.a. in chloride, nitrate and perchlorate media,
320 respectively. These curves can be separated into three regions: the charge-transfer-limited
321 region with initial exponential increase in current density, the mixed kinetics region where
322 diffusion and charge transfer both contribute to the kinetics, and the mass-transfer limited
323 plateaus. The kinetic analysis using a rotating disk electrode can be performed using two
324 correlations in the respective regions: Levich and Koutecký-Levich analysis. The equations to
325 calculate the kinetic parameters via these methods are given as:

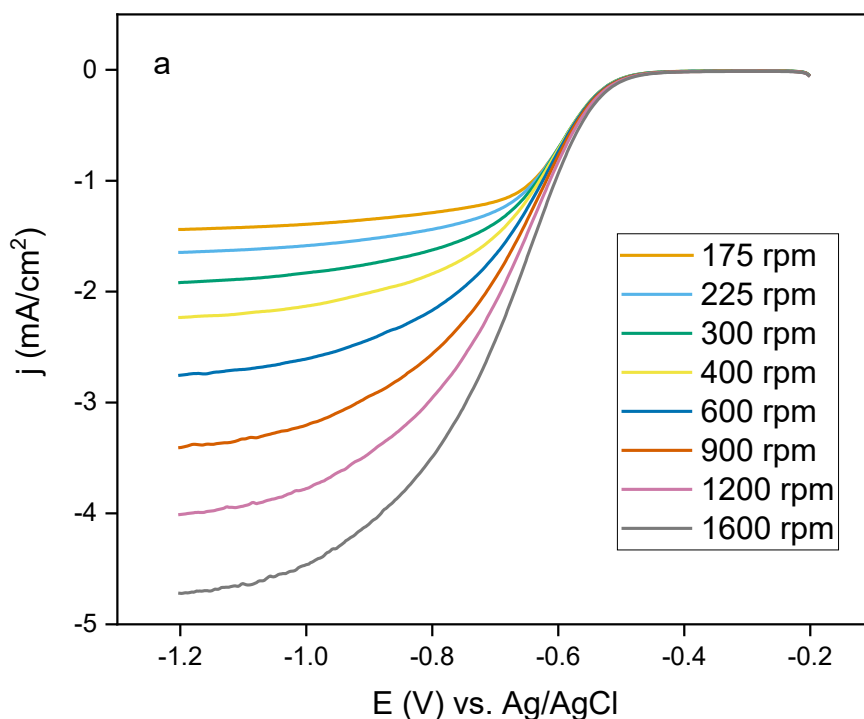
$$326 \quad \frac{1}{i} = \frac{1}{i_k} + \frac{1}{i_l} = \frac{1}{i_k} + \frac{1}{B\omega^{1/2}} \quad (3)$$

$$327 \quad B = 0.62AnFD^{2/3}\nu^{-1/6}C \quad (4)$$

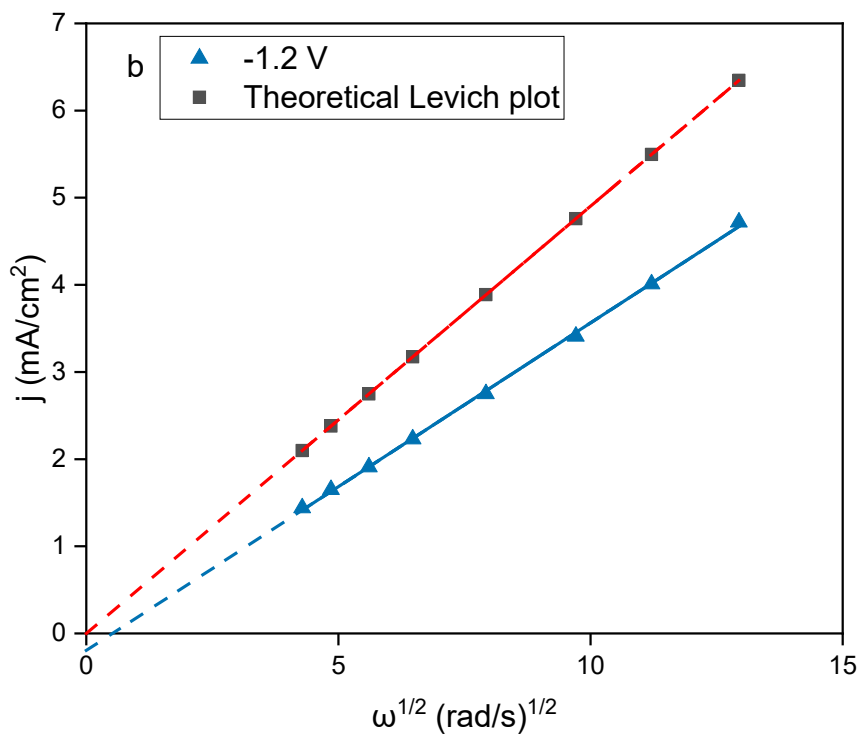
328
$$i_k = nFAkC \quad (5)$$

329
$$i_l = 0.62AnFD^{2/3}\nu^{-1/6}C\sqrt{\omega} \quad (6)$$

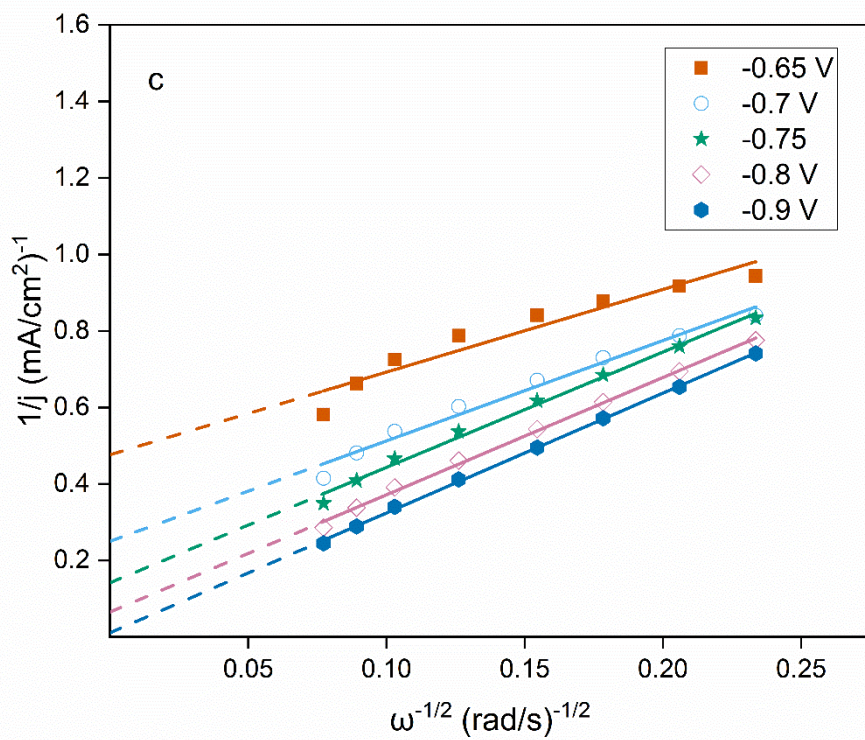
330 The variables for these equations are; n is the number of exchanged electrons, F is the
 331 Faraday constant (96485 C.mol⁻¹), C is the europium concentration (in mol.cm⁻³), A is the
 332 electrode surface area (in cm²), k is the rate constant for electron transfer (in cm.s⁻¹), D is the
 333 diffusion coefficient (in cm².s⁻¹), ν is the potential sweep rate (in V.s⁻¹), α is the charge-transfer
 334 coefficient, n_α is the number of electrons transferred in the rate-determining step, R is the
 335 universal gas constant (8.314 J.mol⁻¹.K⁻¹), T is the absolute temperature (in K), ω is the angular
 336 frequency of rotation (rad.s⁻¹), ν is the kinematic viscosity of the electrolyte (cm².s⁻¹), i_k is the
 337 kinetic current and i_l is the limiting current (in A).



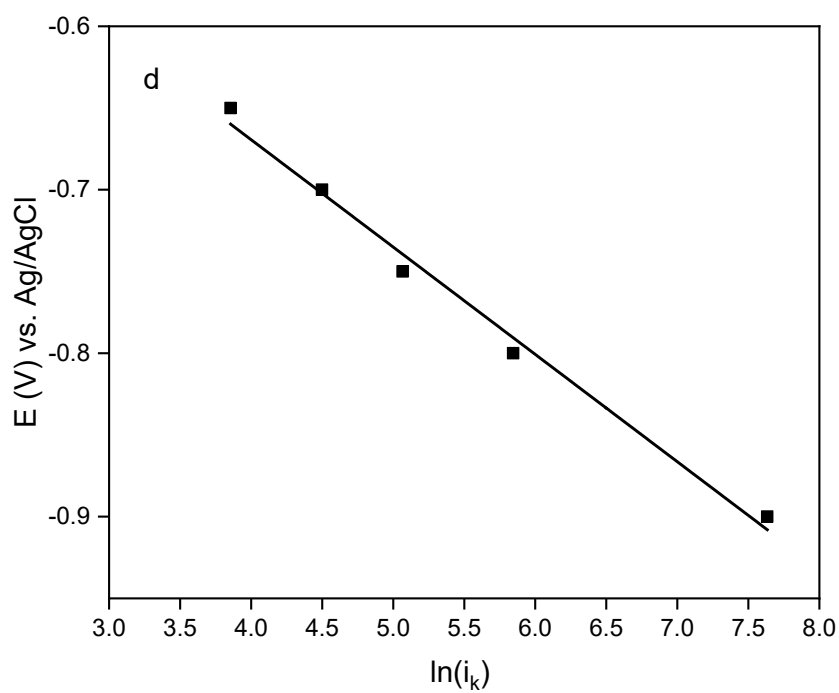
338



339

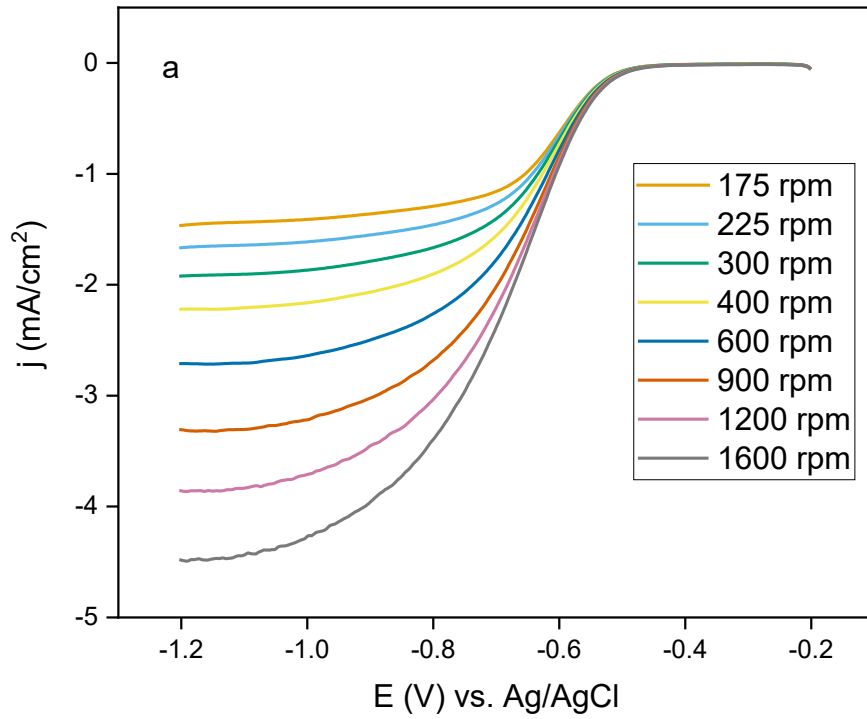


340

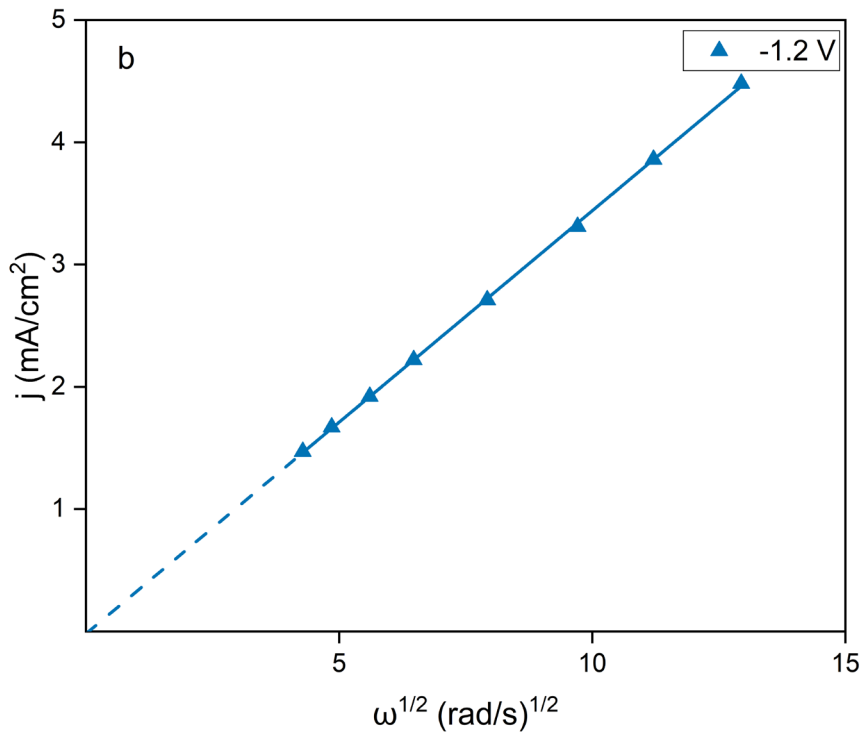


341

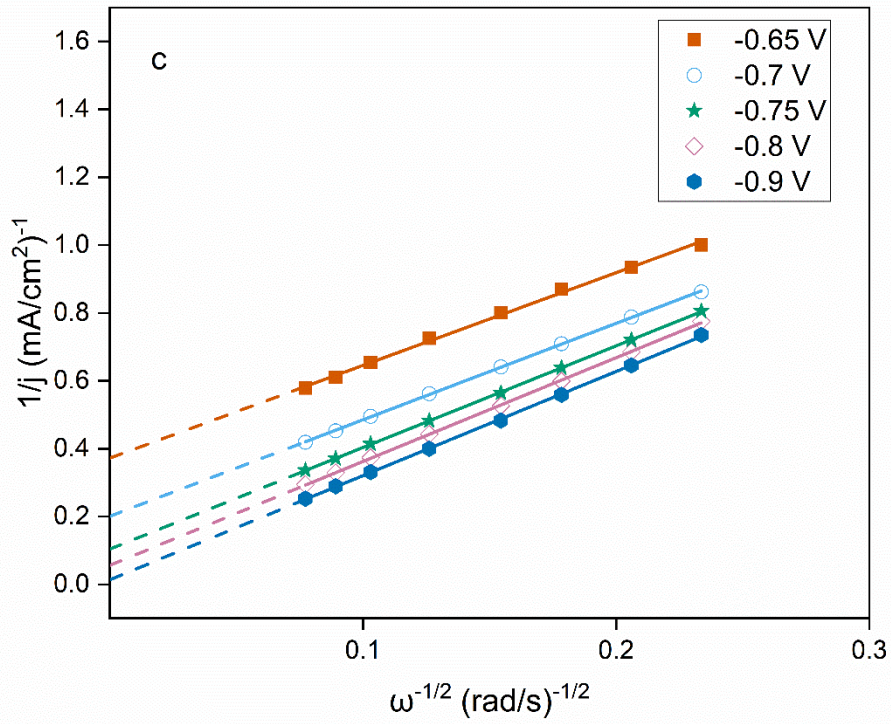
342 Fig. 8. a) Linear sweep voltammogram on a glassy carbon rotating disk electrode in 0.01 mol L⁻¹ Eu³⁺ in 0.1
 343 mol.L⁻¹ CaCl₂ solution at a scan rate of 50 mV.s⁻¹ for rotation speeds 175 – 1600 rpm b) Levich plot and c)
 344 Koutecký – Levich plot at various potentials d) Tafel plot deduced from the Koutecký–Levich analysis



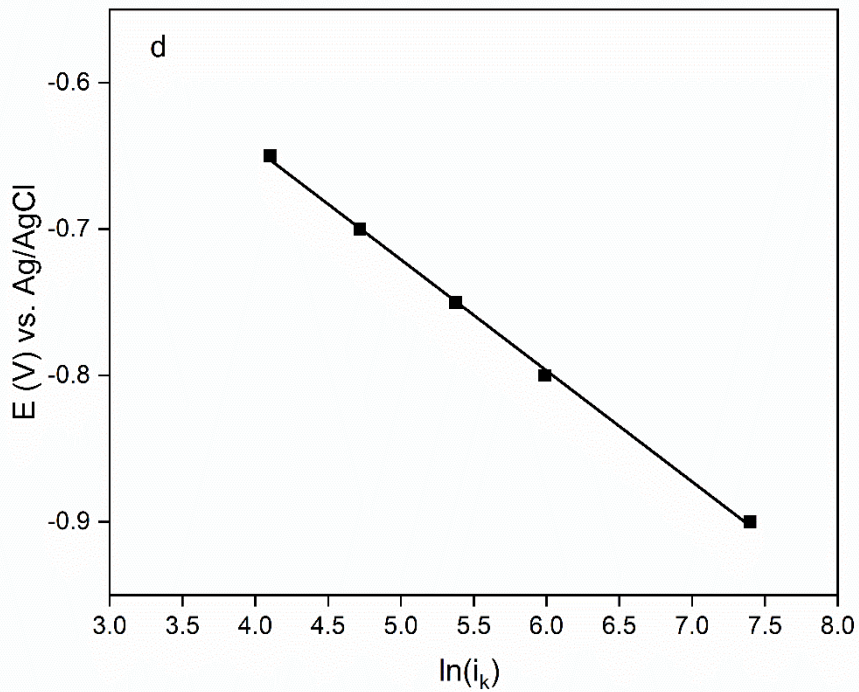
345



346



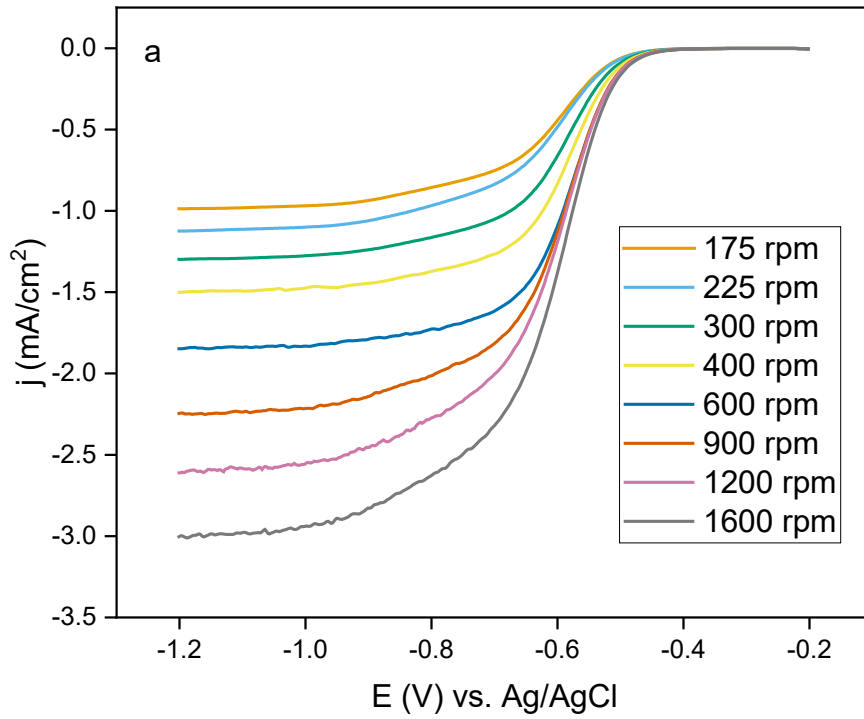
347



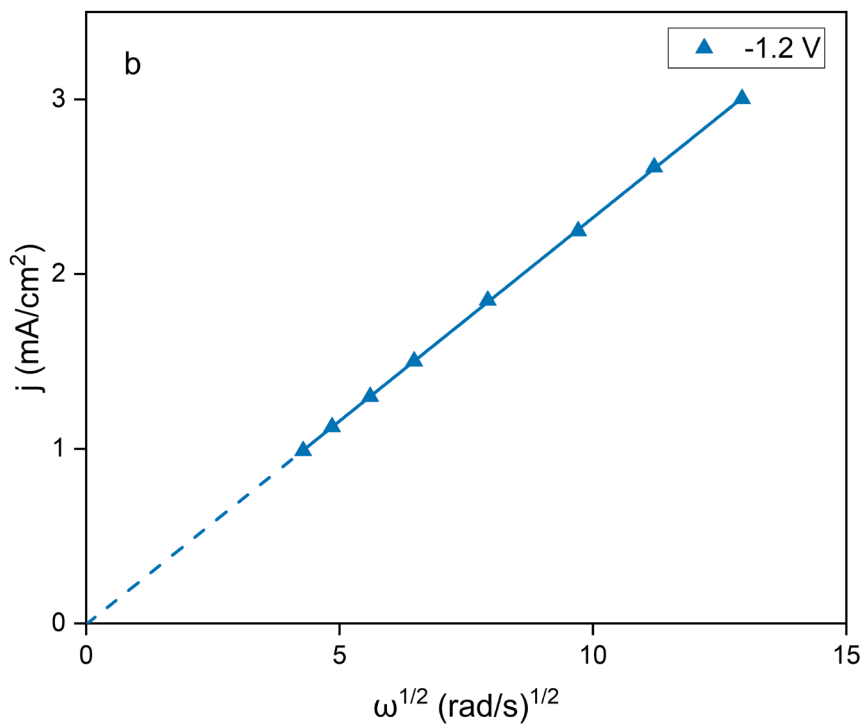
348

349

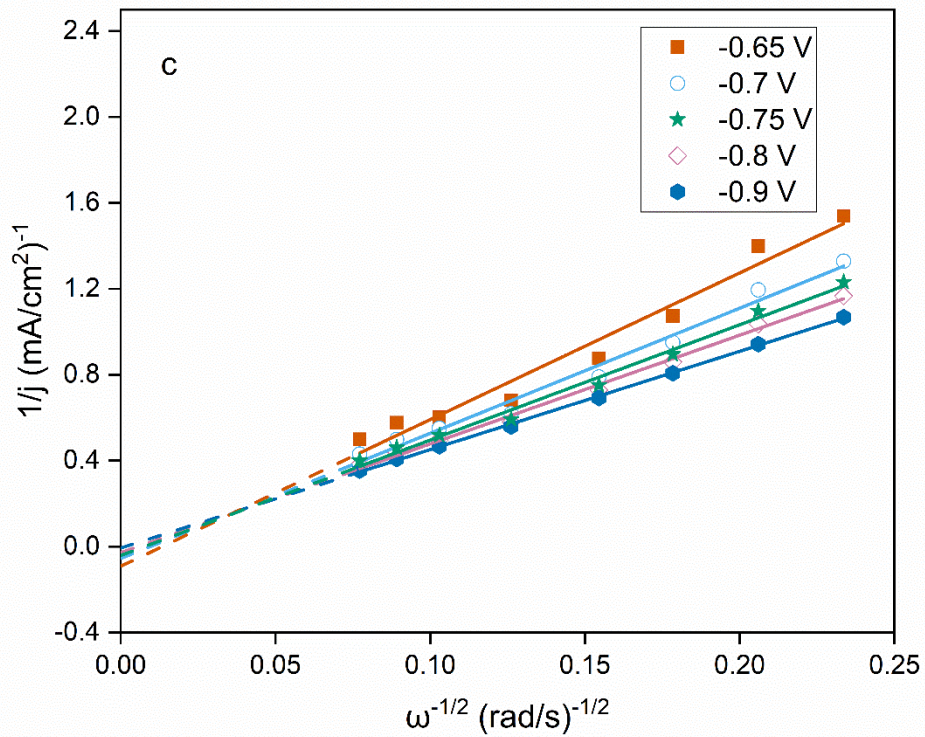
350 Fig. 9. a) Linear sweep voltammogram on a glassy carbon rotating disk electrode in 0.01 mol.L⁻¹ Eu³⁺ in 0.1
 351 mol.L⁻¹ Ca(NO₃)₂ solution at a scan rate of 50 mV s⁻¹ for rotation speeds 175 – 1600 rpm b) Levich plot and c)
 352 Koutecký – Levich plot at various potentials d) Tafel plot deduced from the Koutecký–Levich analysis



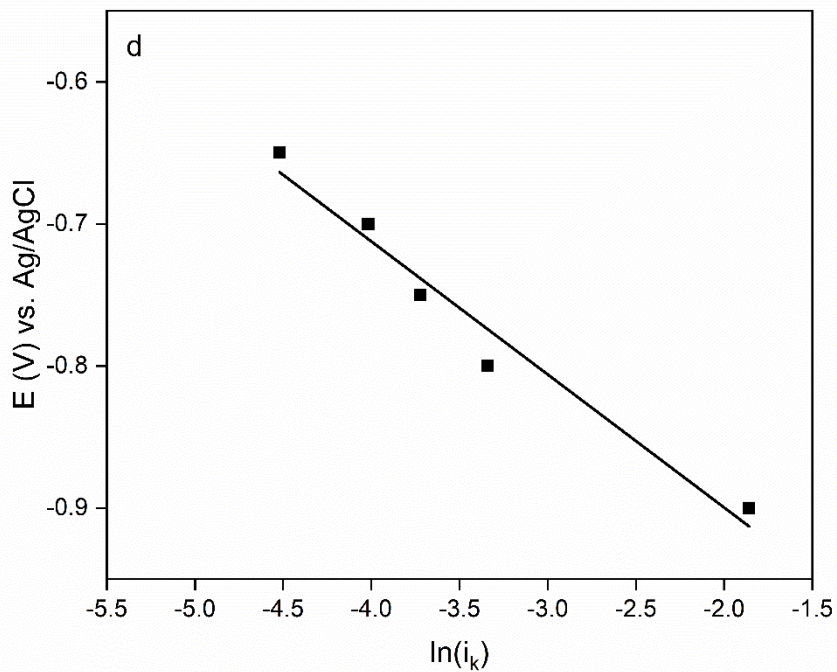
353



354



355



356

357

358 Fig. 10. a) Linear sweep voltammogram on a glassy carbon rotating disk electrode in 0.01 mol.L⁻¹ Eu³⁺ in 1 mol.L⁻¹
 359 ¹ NaClO₄ solution at a scan rate of 50 mV.s⁻¹ for rotation speeds 175 – 1600 rpm b) Levich plot and c) Koutecký
 360 – Levich plot at various potentials.

361 The Levich plots are presented in Fig. 5.b., Fig. 6.b., and Fig. 7.b., and were fitted by linear
362 regression analysis, with the intercepts shown. Based on Eqn. 6, the slope of the Levich plot
363 can be used to calculate the diffusion coefficients. These calculated values are given in Table
364 2. There is no deviation from the linearity in these plots, with linear fitting R^2 values ($R^2 \geq$
365 0.999), proving the mass transport regime at the limiting current. However, it is observed that
366 in chloride medium due to the adsorption of Eu^{3+} ions rather than Eu^{2+} over the electrode
367 surface, the experimental Levich plot deviates from the theoretical one. The kinematic
368 viscosities for the electrolyte solutions were estimated by the literature values reported as
369 $0.00899 \text{ cm}^2 \cdot \text{s}^{-1}$ for $0.1 \text{ mol} \cdot \text{L}^{-1} \text{ Ca}(\text{NO}_3)_2$, $0.00896 \text{ cm}^2 \cdot \text{s}^{-1}$ for $0.1 \text{ mol} \cdot \text{L}^{-1} \text{ CaCl}_2$, and 0.00917
370 $\text{ cm}^2 \cdot \text{s}^{-1}$ for $1 \text{ mol} \cdot \text{L}^{-1} \text{ NaClO}_4$ [21][52]. By using the Levich equation, the diffusion coefficients
371 were calculated with the assumption that the reaction is a one-electron process. For
372 perchlorate medium, the diffusion coefficient values are in the same order of magnitude
373 compared to the earlier calculations from cyclic voltammetry, where the values are slightly
374 higher in less concentrated nitrate ($10.7 \times 10^6 \text{ cm}^2 \cdot \text{s}^{-1}$) and chloride ($11.71 \times 10^6 \text{ cm}^2 \cdot \text{s}^{-1}$)
375 solutions compared to the perchlorate media ($7.28 \times 10^6 \text{ cm}^2 \cdot \text{s}^{-1}$). A variation is observed
376 between diffusion coefficients calculated based on cyclic voltammetry (Randles-Sevcik and
377 simulation) and rotating disk electrode. Values are all in the same order of magnitude and the
378 ratios between the investigated media are consistent over all applied methods. Koutecký-
379 Levich analysis was performed to calculate the rate constant for the charge transfer in all
380 media, and the results are summarized in Table 2.

381

382

383

Table 2. D , α and k values calculated based on Levich and Koutecký-Levich analysis.

Medium	$D \times 10^6$ (cm ² /s)	k (cm/s)	k (cm/s)*
1 mol.L ⁻¹ NaClO ₄	7.28	1.13×10^{-4}	1.6×10^{-4} [38] 2.4×10^{-4} [29]
0.1 mol.L ⁻¹ Ca(NO ₃) ₂	10.7	2.88×10^{-3}	-
0.1 mol.L ⁻¹ CaCl ₂	11.71	2.18×10^{-3}	-

385 *These values are obtained from literature reports.

386 The rate constants were calculated by using equations 3, 4 and 5, where the intercept of the
 387 Koutecký-Levich plot equals to the inverse of the kinetic current. The value for the reference
 388 perchlorate medium was calculated as 1.13×10^{-4} cm.s⁻¹, which is very similar to the literature
 389 values [29,38]. The calculated value being similar to the literature validates that this method
 390 is applicable to the aqueous electrolytes that are studied. It was observed that in nitrate and
 391 chloride media, the rate constant was ten times larger than in perchlorate medium with 2.88
 392 $\times 10^{-3}$ cm.s⁻¹ in nitrate and 2.18×10^{-3} cm.s⁻¹ in chloride solutions. These differences can be
 393 explained by the differences in hydration at different concentrations. In addition to the
 394 differences in hydration of the europium ions and viscosity of the solutions due to the
 395 electrolyte concentration, for nitrate medium, reduction products of nitrate might influence
 396 the electrode reactions [21,56].

397 According to the literature data [27,31], the rate of the electrode process in chloride and
 398 perchlorate solutions should be similar ($k \sim 10^{-4}$ cm.s⁻¹) since inner-sphere complexation and
 399 anion adsorption are not prominent, whereas in nitrate medium an opposite observation is
 400 made. Additionally, it was demonstrated that the first coordination sphere of Eu³⁺ in
 401 perchlorate and chloride solutions solely contains water molecules, even at very high salt

402 concentrations, whereas EuNO_3^{2+} can also form in nitrate medium [43]. Based on a study by
403 Kinard *et al.* [27], the reversibility as a function of supporting electrolytes shows the following
404 trend: $\text{ClO}_4^- < \text{Cl}^- < \text{NO}_3^- < \text{Br}^- < \text{I}^- < \text{SCN}^-$ and the outer-sphere complexes give the same
405 limiting current, indicating similarities in reduction mechanism within this series. Although the
406 differences in complexation could impact the kinetics at higher concentrations, based on
407 these results, the differences in rate constants and diffusion coefficients can be attributed
408 rather to the concentration of these electrolytes.

409 **4. Conclusions**

410

411 The kinetics of the Eu^{3+} to Eu^{2+} reduction reaction were studied in perchlorate, nitrate and
412 chloride media using cyclic voltammetry and linear sweep voltammetry on a rotating disk
413 electrode. The perchlorate medium was selected as a reference condition to explore the
414 methodology, and the kinetics study in the nitrate and chloride electrolytes are explored, to
415 the best of our knowledge, for the first time. The diffusion coefficients were calculated by both
416 cyclic voltammetry and Levich analysis, and these values are in the same order of magnitude
417 and in a good agreement with literature data based on polarographic methods. The reaction
418 is quasi-reversible in all the electrolytes under these chosen experimental conditions, which
419 is confirmed by the difference in peak separation potential. It was proposed that the hydrogen
420 reduction reaction occurs at higher potentials in the perchlorate media and partially overlaps
421 with Eu^{3+} reduction. Koutecký-Levich analysis was performed to retrieve information on the
422 kinetic parameters of the Eu^{3+} reduction for the first time. The rate constants in the different
423 media amount to $1.13 \times 10^{-4} \text{ cm}\cdot\text{s}^{-1}$ for perchlorate, $2.88 \times 10^{-3} \text{ cm}\cdot\text{s}^{-1}$ for nitrate and 2.18×10^{-3}
424 $\text{ cm}\cdot\text{s}^{-1}$ for chloride. Hence, the values for nitrate and chloride differ one order of magnitude.
425 These minor differences in the nitrate and chloride electrolytes can be attributed to

426 differences in concentration and viscosity rather than to the complexation or sluggish kinetics,
427 since the concentrations were low.

428 **Acknowledgements**

429

430 This research was funded by the SCK•CEN Academy (granted to MOA).

431 **References**

432

- 433 [1] L.B. Asprey, B.B. Cunningham, Unusual oxidation states of some actinide and lanthanide elements,
434 *Progress in Inorganic Chemistry* 2 (1960) 267–302. <https://doi.org/10.1002/9780470166031.ch6>.
- 435 [2] P.D. Schumacher, J.L. Doyle, J.O. Schenk, S.B. Clark, Electroanalytical chemistry of lanthanides and
436 actinides, *Rev Anal Chem* 32 (2013) 159–171. <https://doi.org/10.1515/revac-2012-0032>.
- 437 [3] P.G. Eller, R.A. Penneman, Stabilization of actinides and lanthanides in high oxidation states, *Journal of*
438 *The Less-Common Metals* 127 (1987) 19–33. [https://doi.org/10.1016/0022-5088\(87\)90354-7](https://doi.org/10.1016/0022-5088(87)90354-7).
- 439 [4] N.B. Mikheev, L.N. Auerman, I.A. Rumer, A.N. Kamenskaya, M.Z. Kazakevich, The anomalous
440 stabilisation of the oxidation state 2+ of lanthanides and actinides, *Russian Chemical Reviews* 61 (1992)
441 990–998. <https://doi.org/10.1070/rc1992v061n10abeh001011>.
- 442 [5] Payne G. F.; Peterson J. R., Oxidation studies of selected lanthanides in acetonitrile, *Journal of The Less-*
443 *Common Metals* 126 (1986) 371–377.
- 444 [6] M. Gibilaro, L. Massot, P. Chamelot, L. Cassayre, P. Taxil, Electrochemical extraction of europium from
445 molten fluoride media, *Electrochim Acta* 55 (2009) 281–287.
446 <https://doi.org/10.1016/j.electacta.2009.08.052>.
- 447 [7] W. Huang, L. Tian, C. She, F. Jiang, H. Zheng, W. Li, G. Wu, D. Long, Q. Li, Electrochemical behavior of
448 europium(III)-europium(II) in LiF-NaF-KF molten salt, *Electrochim Acta* 147 (2014) 114–120.
449 <https://doi.org/10.1016/j.electacta.2014.08.119>.
- 450 [8] S.A. Kuznetsov, Electrochemical study of stabilization higher oxidation states of d- and f-metals in
451 molten salts, *Int J Electrochem Sci* 11 (2016) 6580–6596. <https://doi.org/10.20964/2016.08.53>.
- 452 [9] M. Yamagata, Y. Katayama, T. Miura, Electrochemical behavior of samarium, europium, and ytterbium
453 in hydrophobic room-temperature molten salt systems, *J Electrochem Soc* 153 (2006) E5–E9.
454 <https://doi.org/10.1149/1.2136088>.
- 455 [10] L.O. de S. Bulhões, T. Rabockai, Electrochemical reduction of lanthanides in propylene carbonate,
456 *Electrochim Acta* 27 (1982) 1071–1073. [https://doi.org/10.1016/0013-4686\(82\)80111-4](https://doi.org/10.1016/0013-4686(82)80111-4).
- 457 [11] C.A. Morais, V.S.T. Ciminelli, Recovery of europium by chemical reduction of a commercial solution of
458 europium and gadolinium chlorides, *Hydrometallurgy* 60 (2001) 247–253.
459 [https://doi.org/10.1016/S0304-386X\(01\)00156-6](https://doi.org/10.1016/S0304-386X(01)00156-6).
- 460 [12] A.R. Willauer, C.T. Palumbo, R. Scopelliti, I. Zivkovic, I. Douair, L. Maron, M. Mazzanti, Stabilization of
461 the oxidation state +IV in siloxide-supported terbium compounds, *Angewandte Chemie - International*
462 *Edition* 59 (2020) 3549–3553. <https://doi.org/10.1002/anie.201914733>.
- 463 [13] A.R. Willauer, C.T. Palumbo, F. Fadaei-Tirani, I. Zivkovic, I. Douair, L. Maron, M. Mazzanti, Accessing the
464 +IV oxidation state in molecular complexes of praseodymium, *J Am Chem Soc* 142 (2020) 5538–5542.
465 <https://doi.org/10.1021/jacs.0c01204>.

- 466 [14] M.O. Arman, B. Geboes, K. Van Hecke, K. Binnemans, T. Cardinaels, Electrochemical oxidation of
467 terbium(III) in aqueous media: influence of supporting electrolyte on oxidation potential and stability, *J*
468 *Appl Electrochem* 52 (2022) 583–593. <https://doi.org/10.1007/s10800-021-01651-0>.
- 469 [15] B. Van Den Bogaert, L. Gheeraert, M.E. Leblebici, K. Binnemans, T. Van Gerven, Photochemical recovery
470 of europium from non-aqueous solutions, *Phys. Chem. Chem. Phys* 18 (2016) 29961–29968.
471 <https://doi.org/10.1039/c6cp06329b>.
- 472 [16] T. Donohue, Photochemical separation of europium from lanthanide mixtures in aqueous solution, *J*
473 *Chem Phys* 67 (1977) 5402–5404. <https://doi.org/10.1063/1.434656>.
- 474 [17] B. Van Den Bogaert, L. Van Meerbeeck, K. Binnemans, T. Van Gerven, Influence of irradiance on the
475 photochemical reduction of europium(III), *Green Chemistry* 18 (2016) 4198–4204.
476 <https://doi.org/10.1039/c6gc00541a>.
- 477 [18] L.F. Qiu, X.H. Kang, T.S. Wang, A study on photochemical separation of rare earths: The separation of
478 europium from an industrial concentrate material of samarium, europium, and gadolinium, *Sep Sci*
479 *Technol* 26 (1991) 199–221. <https://doi.org/10.1080/01496399108050467>.
- 480 [19] T. Hirai, I. Komasaawa, Separation of europium from samarium and gadolinium by combination of
481 electrochemical reduction and solvent extraction, *Journal of Chemical Engineering of Japan* 25 (1992)
482 644–648. <https://doi.org/10.1252/jcej.25.644>.
- 483 [20] S.A. Sayed, K.A. Rabie, I.E. Salama, Studies on europium separation from a middle rare earth
484 concentrate by in situ zinc reduction technique, *Sep Purif Technol* 46 (2005) 145–154.
485 <https://doi.org/10.1016/J.SEPPUR.2005.05.006>.
- 486 [21] M. Van De Voorde, B. Geboes, T. Vander Hoogerstraete, K. Van Hecke, T. Cardinaels, K. Binnemans,
487 Stability of europium(II) in aqueous nitrate solutions, *Dalton Transactions* 48 (2019) 14758–14768.
488 <https://doi.org/10.1039/c9dt03139a>.
- 489 [22] E. Härk, R. Jäger, K. Lust, H. Kasuk, E. Lust, The kinetics of electroreduction of europium(III) cations at
490 bismuth single-crystal electrode, *Journal of Solid State Electrochemistry* 16 (2012) 921–926.
491 <https://doi.org/10.1007/s10008-011-1443-3>.
- 492 [23] M.C. Henstridge, Y. Wang, J.G. Limon-Petersen, E. Laborda, R.G. Compton, An experimental comparison
493 of the Marcus-Hush and Butler-Volmer descriptions of electrode kinetics applied to cyclic voltammetry.
494 The one electron reductions of europium (III) and 2-methyl-2-nitropropane studied at a mercury
495 microhemisphere electrode, *Chem Phys Lett* 517 (2011) 29–35.
496 <https://doi.org/10.1016/j.cplett.2011.10.004>.
- 497 [24] S. Ferro, A. De Battisti, Electrochemistry of the aqueous europium(III)/europium(II) redox couple at
498 conductive diamond electrodes, *Journal of Electroanalytical Chemistry* 533 (2002) 177–180.
499 [https://doi.org/10.1016/S0022-0728\(02\)01073-2](https://doi.org/10.1016/S0022-0728(02)01073-2).
- 500 [25] E.R. Bertelsen, N.C. Kovach, B.G. Trewyn, M.R. Antonio, J.C. Shafer, Electrochemical reduction of
501 europium(III) using tetra-n-octyl diglycolamide functionalized ordered mesoporous carbon
502 microelectrodes, *J Mater Chem C Mater* 8 (2020) 6689–6700. <https://doi.org/10.1039/D0TC00824A>.
- 503 [26] A. Adin, A.G. Sykes, The kinetics of the oxidation of europium(II) with vanadium(III) and chromium(III) in
504 aqueous perchloric acid solutions, *Journal of Chemical Society* (1966) 1230–1236.
- 505 [27] W. Frank Kinard, R.H. Philp, Electrochemical studies of the Eu(III)/(II) reaction by conventional and
506 kalousek polarography, *J Electroanal Chem Interfacial Electrochem* 25 (1970) 373–379.
507 [https://doi.org/10.1016/S0022-0728\(70\)80099-7](https://doi.org/10.1016/S0022-0728(70)80099-7).
- 508 [28] A.G. Atanasyants, A.N. Seryogin, The reaction of the electrochemical reduction $\text{Eu(III)} + e^- \rightarrow \text{Eu(II)}$ in
509 hydrochloric solution, *Hydrometallurgy* 37 (1995) 367–374. [https://doi.org/10.1016/0304-](https://doi.org/10.1016/0304-386X(94)00036-3)
510 [386X\(94\)00036-3](https://doi.org/10.1016/0304-386X(94)00036-3).

- 511 [29] T. Rabockai, I. Jordan, Electrochemistry of europium in aqueous and aqueous formamide solutions,
512 Anal Lett 7 (1974) 647–658. <https://doi.org/10.1080/00032717408059025>.
- 513 [30] T. Rabockai, The influence of temperature on the diffusion coefficient of europium in aqueous
514 formamide solutions, Electrochim Acta 22 (1977) 489–490. [https://doi.org/10.1016/0013-4686\(77\)85106-2](https://doi.org/10.1016/0013-4686(77)85106-2).
- 516 [31] M. Zelić, Electrochemical reduction of europium (3+) at increasing concentrations of different salts. Part
517 I. Voltammetric measurements, Croatica Chemica Acta 76 (2003) 241–248.
- 518 [32] T. Rabockai, Electrochemical reduction of ytterbium in perchloric media, J Electroanal Chem Interfacial
519 Electrochem 76 (1977) 83–89. [https://doi.org/https://doi.org/10.1016/S0022-0728\(77\)80008-9](https://doi.org/https://doi.org/10.1016/S0022-0728(77)80008-9).
- 520 [33] B. Timmer, M. Sluyters-Rehbach, J.H. Sluyters, On the impedance of galvanic cells, J Electroanal Chem
521 14 (1967) 181–191. [https://doi.org/10.1016/0022-0728\(67\)80067-6](https://doi.org/10.1016/0022-0728(67)80067-6).
- 522 [34] A. Kumari, M.K. Jha, D.D. Pathak, S. Chakravarty, J. Lee, Processes developed for the separation of
523 europium (Eu) from various resources, Separation and Purification Reviews 48 (2019) 91–121.
524 <https://doi.org/10.1080/15422119.2018.1454959>.
- 525 [35] M. Van de Voorde, K. Van Hecke, K. Binnemans, T. Cardinaels, Supported ionic liquid phases for the
526 separation of samarium and europium in nitrate media: Towards purification of medical samarium-153,
527 Sep Purif Technol 232 (2020). <https://doi.org/10.1016/j.seppur.2019.115939>.
- 528 [36] M. Van de Voorde, K. Van Hecke, K. Binnemans, T. Cardinaels, Separation of samarium and europium
529 by solvent extraction with an undiluted quaternary ammonium ionic liquid: towards high-purity medical
530 samarium-153, RSC Adv 8 (2018) 20077–20086. <https://doi.org/10.1039/C8RA03279C>.
- 531 [37] A. Yörükoğlu, İ. Girgin, Recovery of europium by electrochemical reduction from sulfate solutions,
532 Hydrometallurgy 63 (2002) 85–91. [https://doi.org/10.1016/S0304-386X\(01\)00215-8](https://doi.org/10.1016/S0304-386X(01)00215-8).
- 533 [38] T. Rabockai, L.O. De S. Bulhões, L.O. Luis, Electrochemical reduction of Eu³⁺ in aqueous ethylene glycol
534 solutions, Electrochim Acta 25 (1980) 1041–1042. [https://doi.org/10.1016/0013-4686\(80\)87012-5](https://doi.org/10.1016/0013-4686(80)87012-5).
- 535 [39] C. Jagadeeswara Rao, K.A. Venkatesan, K. Nagarajan, T.G. Srinivasan, P.R. Vasudeva Rao,
536 Electrochemical behavior of europium (III) in N-butyl-N-methylpyrrolidinium
537 bis(trifluoromethylsulfonyl)imide, Electrochim Acta 54 (2009) 4718–4725.
538 <https://doi.org/10.1016/j.electacta.2009.03.074>.
- 539 [40] M. Cetnarska, J. Stroka, Electrode processes of the Eu(III)/Eu(II) system in water +
540 hexamethylphosphortriamide mixtures, J Electroanal Chem Interfacial Electrochem 234 (1987) 263–
541 275. [https://doi.org/10.1016/0022-0728\(87\)80177-8](https://doi.org/10.1016/0022-0728(87)80177-8).
- 542 [41] E.H. Borai, A.M. Shahr El-Din, E.M. El Afifi, R.F. Aglan, M.M. Abo-Aly, Subsequent separation and
543 selective extraction of thorium (IV), iron (III), zirconium (IV) and cerium (III) from aqueous sulfate
544 medium, South African Journal of Chemistry 69 (2016) 148–156. <https://doi.org/10.17159/0379-4350/2016/v69a18>.
- 546 [42] T. Rabockai, L.O. Luis, Electrochemical reduction of Eu³⁺ in aqueous ethylene glycol solutions,
547 Electrochim Acta 25 (1980) 1041–1042. [https://doi.org/10.1016/0013-4686\(80\)87012-5](https://doi.org/10.1016/0013-4686(80)87012-5).
- 548 [43] F. Tanaka, S. Yamashita, Luminescence lifetimes of aqueous europium chloride, nitrate, sulfate, and
549 perchlorate solutions. studies on the nature of the inner coordination sphere of the europium(III) ion,
550 Inorg Chem 23 (1984) 2044–2046. <https://doi.org/10.1021/ic00182a013>.
- 551 [44] J.A. Rard, Chemistry and thermodynamics of europium and some of its simpler inorganic compounds
552 and aqueous species, Chem Rev 85 (1985) 555–582. <https://doi.org/10.1021/cr00070a003>.
- 553 [45] J. Garcia, M.J. Allen, Developments in the coordination chemistry of europium(II), Eur J Inorg Chem 29
554 (2012) 4550–4563. <https://doi.org/10.1002/ejic.201200159>.

- 555 [46] S. Friesen, S. Krickl, M. Luger, A. Nazet, G. Hefter, R. Buchner, Hydration and ion association of La³⁺ and
556 Eu³⁺ salts in aqueous solution, *Physical Chemistry Chemical Physics* 20 (2018) 8812–8821.
557 <https://doi.org/10.1039/c8cp00248g>.
- 558 [47] A.J. Bard, L.R. Faulkner, *Electrochemical methods fundamentals and applications*, John Wiley & Sons,
559 Ltd, 2001.
- 560 [48] A. Capucciati, A. Burato, C. Bersani, S. Protti, A. Profumo, D. Merli, Electrochemical Behavior and
561 Voltammetric Determination of Two Synthetic Aroyl Amides Opioids, *Chemosensors* 11 (2023) 198.
562 <https://doi.org/10.3390/CHEMOSENSORS11030198/S1>.
- 563 [49] J.H. Brown, Development and Use of a Cyclic Voltammetry Simulator To Introduce Undergraduate
564 Students to Electrochemical Simulations, *J Chem Educ* 92 (2015) 1490–1496.
565 https://doi.org/10.1021/ACS.JCHEMED.5B00225/SUPPL_FILE/ED5B00225_SI_001.XLS.
- 566 [50] E. Steeman, E. Temmerman, F. Verbeek, Electrochemical reduction of the lanthanide ions: Part I. First
567 reduction step of ytterbium(III) in acidic 1 M NaClO₄ solution, *J Electroanal Chem Interfacial*
568 *Electrochem* 89 (1978) 97–111. [https://doi.org/10.1016/S0022-0728\(78\)80035-7](https://doi.org/10.1016/S0022-0728(78)80035-7).
- 569 [51] A.A. Shaikh, M. Begum, A.H. Khan, M.Q. Ehsan, Cyclic voltammetric studies of the redox behavior of
570 iron(III)-vitamin B6 complex at carbon paste electrode, *Russian Journal of Electrochemistry* 42 (2006)
571 620–625. <https://doi.org/10.1134/S1023193506060048>.
- 572 [52] D.A.C. da Silva, M.J. Pinzón C, A. Messias, E.E. Fileti, A. Pascon, D. V. Franco, L.M. Da Silva, H.G. Zanin,
573 Effect of conductivity, viscosity, and density of water-in-salt electrolytes on the electrochemical
574 behavior of supercapacitors: molecular dynamics simulations and in situ characterization studies,
575 *Mater. Adv* 3 (2022) 611–623. <https://doi.org/10.1039/d1ma00890k>.
- 576 [53] S. Treimer, A. Tanga, D.C. Johnson, A consideration of the application of Koutecký-Levich plots in the
577 diagnoses of charge-transfer mechanisms at rotated disk electrodes, *Electroanalysis* 14 (2002) 165–171.
578 [https://doi.org/10.1002/1521-4109\(200202\)14:3<165::AID-ELAN165>3.0.CO;2-6](https://doi.org/10.1002/1521-4109(200202)14:3<165::AID-ELAN165>3.0.CO;2-6).
- 579 [54] R.R. Rao, S.B. Milliken, S.L. Robinson, C.K. Mann, Anodic oxidation of lithium, cadmium, silver, and
580 tetrabutylammonium nitrates, *Anal Chem* 42 (1970) 1076–1080. <https://doi.org/10.1021/ac60291a006>.
- 581 [55] H. Mishima, T. Iwasita, V.A. Macagno, M.C. Giordano, The electrochemical oxidation of nitrate ion on
582 platinum from silver nitrate in acetonitrile solutions—I. kinetic analysis, *Electrochim Acta* 18 (1973)
583 287–292. [https://doi.org/10.1016/0013-4686\(73\)80030-1](https://doi.org/10.1016/0013-4686(73)80030-1).
- 584 [56] M. Štulíková, Is nitrate really an inert electrolyte? A brief review, *Talanta* 38 (1991) 805–807.
585 [https://doi.org/10.1016/0039-9140\(91\)80205-e](https://doi.org/10.1016/0039-9140(91)80205-e).
- 586
- 587
- 588